

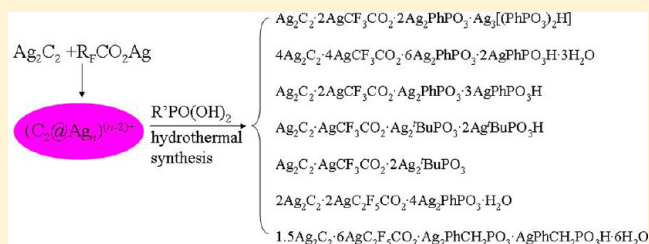
## Silver(I) Multiple Salts Assembled with Phosphonate, Perfluorocarboxylate, and the Multinuclear Silver-Ethynediide Supramolecular Synthron

Ting Hu and Thomas C. W. Mak\*

Department of Chemistry and Center of Novel Functional Molecules, The Chinese University of Hong Kong, Shatin, New Territories, Hong Kong SAR, People's Republic of China

## S Supporting Information

**ABSTRACT:** A series of seven new silver(I) multiple salts containing  $C_2^{2-}$  (ethynediide, acetylenediide), phosphonate, and perfluorocarboxylate ligands,  $Ag_2C_2 \cdot 2AgCF_3CO_2 \cdot 2Ag_2PhPO_3 \cdot Ag_3[(PhPO_3)_2H]$  (1),  $4Ag_2C_2 \cdot 4AgCF_3CO_2 \cdot 6Ag_2PhPO_3 \cdot 2AgPhPO_3H \cdot 3H_2O$  (2),  $Ag_2C_2 \cdot 2AgCF_3CO_2 \cdot Ag_2PhPO_3 \cdot 3AgPhPO_3H$  (3),  $Ag_2C_2 \cdot AgCF_3CO_2 \cdot Ag_2^tBuPO_3 \cdot 2Ag^tBuPO_3H$  (4),  $Ag_2C_2 \cdot AgCF_3CO_2 \cdot 2Ag_2^tBuPO_3$  (5),  $2Ag_2C_2 \cdot 2AgC_2F_5CO_2 \cdot 4Ag_2PhPO_3 \cdot H_2O$  (6), and  $1.5Ag_2C_2 \cdot 6AgC_2F_5CO_2 \cdot Ag_2PhCH_2PO_3 \cdot AgPhCH_2PO_3H \cdot 6H_2O$  (7), have been synthesized under hydrothermal conditions by varying the types of phosphonic and perfluorocarboxylic acid employed, as well as the mole ratios of the reactants. In compound 1,  $C_2@Ag_9$  building units (each with a  $C_2^{2-}$  species located inside a  $Ag_9$  monocapped distorted square antiprism) are consolidated by trifluoroacetate ligands and interconnected by phenylphosphonate groups to form a two-dimensional coordination network. Compound 2 is composed of two kinds of  $C_2@Ag_6$  silver cages that are fused together to form an argentophilic chain; such chains are in turn further linked by the phenylphosphonate ligands into a two-dimensional network. Compound 3 also has a layer structure, whose core is a centrosymmetric  $(C_2)_2@Ag_{18}$  aggregate. In compound 4, centrosymmetric  $(C_2)_2@Ag_{14}$  aggregates are cross-linked into a coordination layer, and such layers are further assembled into a three-dimensional supramolecular architecture via hydrogen bonding. Compound 5 has an argentophilic layer structure generated from the fusion and linkage of  $C_2@Ag_8$  cages. Compound 6 exhibits an argentophilic layer structure in which the basic building unit is an unusual silver(I) aggregate composed of four different kinds of  $C_2@Ag_6$  cages. The crystal structure of compound 7 is a three-dimensional coordination network, in which the coordination chains containing two kinds of  $C_2@Ag_8$  single cages are bridged by aqua ligands.



## ■ INTRODUCTION

Over the past decade, we have established the identity and utility of metal–ligand silver-ethynediide and silver-ethynide supramolecular synthons, which include  $C_2@Ag_n$  ( $n = 6–9$ ),<sup>1</sup>  $Ag_4C\equiv C-C\equiv CAg_4$ ,<sup>2</sup> and  $R-C\equiv CAg_n$  ( $n = 3, 4, 5$ ;  $R = \text{alkyl, aryl, heteroaryl}$ ),<sup>3</sup> as multinuclear structure-building units. Their application in the construction of organosilver(I) coordination networks<sup>3b,d,4</sup> and high-nuclearity clusters<sup>2c,3f,g,4a,5</sup> have been explored by us<sup>1,4a,6</sup> and other groups.<sup>2c,4b,5,7</sup>

Metal phosphonates have attracted much interest in the past two decades due to their structural diversity and potential application in the areas of ion exchange,<sup>8</sup> magnetism,<sup>9</sup> catalysis,<sup>10</sup> molecular recognition,<sup>11</sup> proton conductivity,<sup>12</sup> and photochemistry.<sup>13</sup> Our recent successful combination of phosphonate ligands with the *tert*-butylethynide supramolecular synthon  $^tBu-C\equiv CAg_n$  for the synthesis of high-nuclearity silver(I) clusters<sup>14</sup> prompted us to investigate the potential of an analogous synthetic strategy based on the silver-ethynediide supramolecular synthon  $C_2@Ag_n$ . However, the introduction of phosphonate into an aqueous system containing silver ethynediide generally afforded a precipitate, which could not be recrystallized for structural characterization. On the other

hand, our previous studies have demonstrated that hydrothermal synthesis is a viable method for the generation of crystalline  $Ag_2C_2$ -containing compounds for structural characterization.<sup>1,15</sup> Following this lead, we have conducted a systematic investigation on the hydrothermal synthesis and structural characterization of a new series of silver(I) ethynediide multiple salts with the incorporation of perfluorocarboxylate and alkyl- and aryl-phosphonate ligands,  $Ag_2C_2 \cdot 2AgCF_3CO_2 \cdot 2Ag_2PhPO_3 \cdot Ag_3[(PhPO_3)_2H]$  (1),  $4Ag_2C_2 \cdot 4AgCF_3CO_2 \cdot 6Ag_2PhPO_3 \cdot 2AgPhPO_3H \cdot 3H_2O$  (2),  $Ag_2C_2 \cdot 2AgCF_3CO_2 \cdot Ag_2PhPO_3 \cdot 3AgPhPO_3H$  (3),  $Ag_2C_2 \cdot AgCF_3CO_2 \cdot Ag_2^tBuPO_3 \cdot 2Ag^tBuPO_3H$  (4),  $Ag_2C_2 \cdot AgCF_3CO_2 \cdot 2Ag_2^tBuPO_3$  (5),  $2Ag_2C_2 \cdot 2AgC_2F_5CO_2 \cdot 4Ag_2PhPO_3 \cdot H_2O$  (6), and  $1.5Ag_2C_2 \cdot 6AgC_2F_5CO_2 \cdot Ag_2PhCH_2PO_3 \cdot AgPhCH_2PO_3H \cdot 6H_2O$  (7).

## ■ EXPERIMENTAL SECTION

**Reagents and Instruments.** All chemicals obtained from commercial sources were of analytically pure grade and used without further purification: silver nitrate (RFCL, 99.9%), silver trifluoroacetate



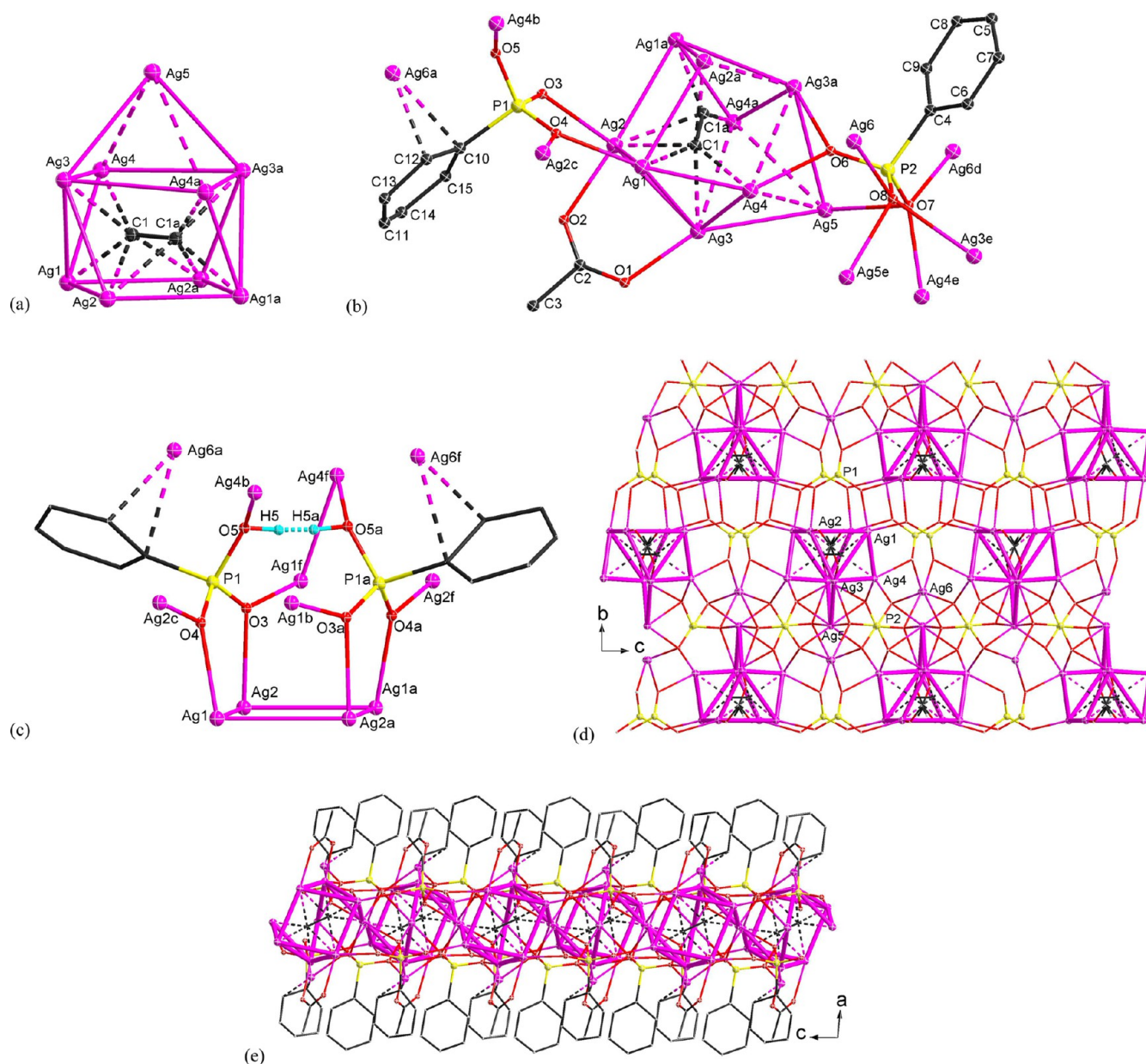


**Figure 1.** (a) The  $C_2@Ag_9$  building block of **1** in the shape of a distorted monocapped square antiprism.  $Ag\cdots Ag$  distances longer than  $3.4 \text{ \AA}$  (twice the van der Waals radius of silver) are represented by broken lines. Selected bond lengths and distances [ $\text{\AA}$ ]:  $C1\equiv C1a$   $1.248(2)$ ,  $Ag\cdots Ag$   $2.773(8)$ – $3.378(9)$ . (b) Asymmetric unit in the crystal structure of **1**, showing the  $C_2@Ag_9$  cage, the coordination modes of the trifluoroacetate and phosphonate groups, and the  $\eta^2$ -coordination of the phenyl group to  $Ag6$ . The F and H atoms are omitted for clarity. (c) The coordination mode of the P1 group, showing the  $[C_6H_5PO_3\cdots H\cdots O_3PC_6H_5]^{3-}$  assembly. (d) Layer structure of **1** viewed along the  $a$  axis, in which the  $C_2@Ag_9$  cages are linked by phosphonate groups. The phenyl moieties, H, and F atoms are omitted for clarity. (e) Layer structure of **1** viewed along the  $b$  axis. The H and F atoms are omitted for clarity. Symmetry codes: (a)  $1-x, y, 1.5-z$ ; (b)  $1-x, 1-y, 2-z$ ; (c)  $x, 1-y, 0.5+z$ ; (d)  $x, -y, -0.5+z$ ; (e)  $1-x, -y, 2-z$ ; (f)  $x, 1-y, -0.5+z$ ; (g)  $1-x, 1-y, 1-z$ .

(ACROS, 98%), silver pentafluoropropionate (Sigma-Aldrich, 98%), *tert*-butylphosphonic acid (ACROS, 98%), phenylphosphonic acid (Strem Chemicals, 98%), benzylphosphonic acid (ACROS, 98%), and silver trifluoroacetate (Sigma-Aldrich, 98%). IR spectra were recorded on KBr pellets at room temperature on a Nicolet Impact 420 FT-IR spectrometer in the range of  $4000\text{--}400 \text{ cm}^{-1}$  at a resolution of  $2 \text{ cm}^{-1}$ . Elemental analysis (C, H, N) was performed by the Analysis and Testing Center at Shanghai Institute of Organic Chemistry, Chinese Academy of Sciences. Melting points in  $^\circ\text{C}$  (uncorrected) were measured with a Reichert apparatus.  $Ag_2C_2$  was prepared as described previously.<sup>16</sup>

Caution!  $Ag_2C_2$  is highly explosive in the dry state and should be stored in the wet form at  $-10 \text{ }^\circ\text{C}$  in the dark, and only a small quantity is to be used for subsequent synthesis.

$Ag_2C_2\cdot 2AgCF_3CO_2\cdot 2Ag_2PhPO_3\cdot Ag_3[(PhPO_3)_2H]$  (**1**). Moist  $Ag_2C_2$  ( $\sim 100 \text{ mg}$ ) was added to a concentrated aqueous solution ( $1 \text{ mL}$ ) of  $AgCF_3CO_2$  ( $0.44 \text{ g}$ ,  $2 \text{ mmol}$ ) and  $AgBF_4$  ( $0.380 \text{ g}$ ,  $2 \text{ mmol}$ ) in a beaker, and the mixture was stirred until the solution was saturated. The excess  $Ag_2C_2$  was filtered off, and phenylphosphonic acid ( $60 \text{ mg}$ ) was then added to the filtrate. The resulting suspension was placed in a  $25 \text{ mL}$  Teflon-lined stainless steel reaction vessel and subjected to hydrothermal conditions at  $120 \text{ }^\circ\text{C}$  for  $36 \text{ h}$ , and subsequently cooled to room temperature at  $4 \text{ }^\circ\text{C/h}$ . Colorless sheet-like crystals of **1** were isolated in 73% yield. Mp (decomp.):  $290.3\text{--}310.6 \text{ }^\circ\text{C}$ . IR:  $\nu = 2082 \text{ cm}^{-1}$  ( $w, \nu_{C\equiv C}$ ). Anal. Calcd for  $C_{30}H_{21}Ag_{11}F_6O_{16}P_4$  ( $M_r = 2061.92$ ): C, 17.48; H, 1.03. Found: C, 17.47; H, 1.25.

$4Ag_2C_2\cdot 4AgCF_3CO_2\cdot 6Ag_2PhPO_3\cdot 2AgPhPO_3\cdot 3H_2O$  (**2**). Compound **2** was synthesized in a manner similar to that of compound **1** using a

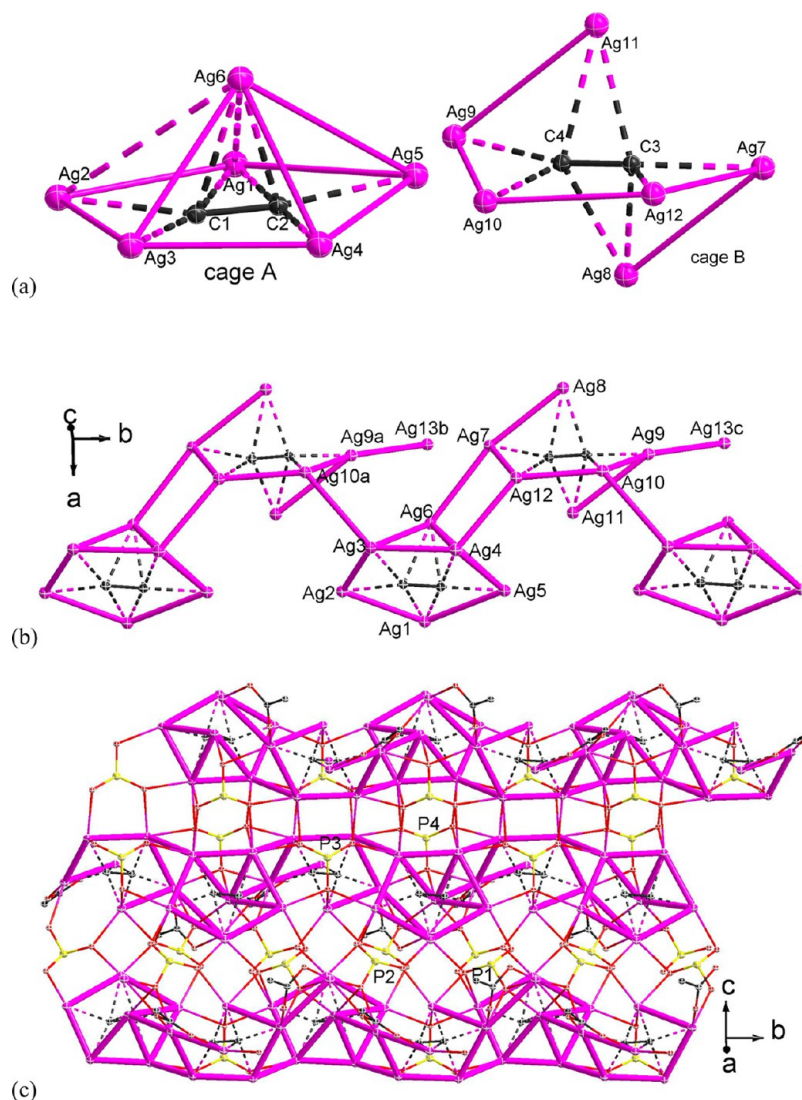


**Figure 2.** (a) Pentagonal pyramidal silver cage A and cage B composed of a pentagonal bipyramid with a missing equatorial vertex, each with an encapsulated  $C_2^{2-}$  ligand, in complex **2**. Edges of cage A longer than 3.4 Å (twice the van der Waals radius of silver) are represented by broken lines. Selected bond lengths and distances [Å]: C1≡C2 1.24(1), C3≡C4 1.23(1), Ag⋯Ag 2.841(1)–3.341(1). (b) Perspective view of silver(I) zigzag chain constructed from two kinds of silver cages connected by argentophilic interactions. (c) Two-dimensional coordination architecture generated from the linkage of silver(I) chains by phosphonate groups. Symmetry codes: (a)  $x, -1 + y, z$ ; (b)  $0.5 - x, 0.5 + y, 0.5 - z$ ; (c)  $0.5 - x, 1.5 + y, 0.5 - z$ .

doubled amount of moist  $Ag_2C_2$ , that is, 200 mg instead of 100 mg. Colorless block-like crystals of **2** were isolated in 63% yield. Compound **2** turns black above 280 °C. IR:  $\nu = 2065\text{ cm}^{-1}$  ( $w, \nu_{C\equiv C}$ ). Anal. Calcd for  $C_{64}H_{48}Ag_{26}F_{12}O_{35}P_8$  ( $M_r = 4657.40$ ): C, 16.51; H, 1.04. Found: C, 16.31; H, 1.07.

$Ag_2C_2 \cdot 2AgCF_3CO_2 \cdot Ag_2PhPO_3 \cdot 3AgPhPO_3H$  (**3**). Compound **3** was synthesized in a manner similar to that of compound **1** using 80 mg of phenylphosphonic acid instead of 60 mg. Colorless rhombus-like crystals of **3** were isolated in 63% yield. Mp (decomp.): 260.6–272.2 °C. IR:  $\nu = 2083\text{ cm}^{-1}$  ( $w, \nu_{C\equiv C}$ ). Anal. Calcd for  $C_{30}H_{23}Ag_9F_6O_{16}P_4$  ( $M_r = 1848.20$ ): C, 19.50; H, 1.25. Found: C, 19.57; H, 1.13.

$Ag_2C_2 \cdot AgCF_3CO_2 \cdot Ag_2^tBuPO_3 \cdot 2Ag^tBuPO_3H$  (**4**). Compound **4** was synthesized in a manner similar to that of compound **1** using *tert*-butylphosphonic acid (60 mg) instead of phenylphosphonic acid (60 mg). Colorless hexagonal-like crystals of **4** were isolated in 81% yield. Compound **4** decomposes above 340 °C. IR:  $\nu = 2079\text{ cm}^{-1}$  ( $w, \nu_{C\equiv C}$ ). Anal. Calcd for  $C_{16}H_{29}Ag_7F_3O_{11}P_3$  ( $M_r = 1302.39$ ): C, 14.76; H, 2.24. Found: C, 14.66; H, 2.37.

$Ag_2C_2 \cdot AgCF_3CO_2 \cdot 2Ag_2^tBuPO_3$  (**5**). Compound **5** was synthesized in a manner similar to that of compound **1** using *tert*-butylphosphonic acid

(40 mg) instead of phenylphosphonic acid (60 mg). Colorless plate-like crystals of **5** were isolated in 81% yield. Compound **5** decomposes above 360 °C. IR:  $\nu = 2075\text{ cm}^{-1}$  ( $w, \nu_{C\equiv C}$ ). Anal. Calcd for  $C_{12}H_{18}Ag_7F_3O_8P_2$  ( $M_r = 1164.29$ ): C, 12.38; H, 1.56. Found: C, 12.25; H, 1.67.

$2Ag_2C_2 \cdot 2AgC_2F_5CO_2 \cdot 4Ag_2PhPO_3 \cdot H_2O$  (**6**). Moist  $Ag_2C_2$  (~100 mg) was added to a concentrated aqueous solution (1 mL) of  $AgC_2F_5CO_2$  (0.44 g, 2 mmol) and  $AgBF_4$  (0.380 g, 2 mmol) in a beaker, and the mixture was stirred until the solution was saturated. The excess  $Ag_2C_2$  was filtered off, and then phenylphosphonic acid (55 mg) was added to the filtrate. The resulted suspension was placed in a 25 mL Teflon-lined stainless steel reaction vessel and subjected to hydrothermal conditions at 120 °C for 36 h, and subsequently cooled to room temperature at 4 °C/h. Colorless block-like crystals of **6** were isolated in 51% yield. Compound **6** decomposes above 320 °C. IR:  $\nu = 2085\text{ cm}^{-1}$  ( $w, \nu_{C\equiv C}$ ). Anal. Calcd for  $C_{68}H_{44}Ag_{28}F_{20}O_{34}P_8$  ( $M_r = 5053.15$ ): C, 16.16; H, 0.86. Found: C, 16.47; H, 1.15.

$1.5Ag_2C_2 \cdot 6AgC_2F_5CO_2 \cdot Ag_2PhCH_2PO_3 \cdot AgPhCH_2PO_3H \cdot 6H_2O$  (**7**). Moist  $Ag_2C_2$  (~100 mg) was added to a concentrated aqueous solution (1 mL) of  $AgC_2F_5CO_2$  (0.44 g, 2 mmol) and  $AgBF_4$  (0.380 g, 2 mmol) in a beaker, and the mixture was stirred until the solution was



saturated. The excess  $\text{Ag}_2\text{C}_2$  was filtered off, and then benzylphosphonic acid (35 mg) was added to the filtrate. The resulted suspension was placed in a 25 mL Teflon-lined stainless steel reaction vessel and subjected to hydrothermal conditions at 120 °C for 36 h, and subsequently cooled to room temperature at 4 °C/h. Colorless plate-like crystals of **7** were isolated in 58% yield. Compound **7** decomposes above 305 °C. IR:  $\nu = 2085\text{ cm}^{-1}$  (w,  $\nu_{\text{C}\equiv\text{C}}$ ). Anal. Calcd for  $\text{C}_{35}\text{H}_{27}\text{Ag}_{12}\text{F}_{30}\text{O}_{24}\text{P}_2$  ( $M_r = 2757.85$ ): C, 15.24; H, 0.99. Found: C, 15.44; H, 1.05.

**Single-Crystal Structure Determination.** Crystal data were collected on a Bruker Smart Apex II CCD diffractometer with Mo  $K\alpha$  radiation ( $\lambda = 0.71073\text{ \AA}$ ) at 293(2) K. The intensities were corrected for Lorentz and polarization factors, as well as for absorption by the multiscan method.<sup>17</sup> The structures were solved by the direct method and refined by full-matrix least-squares fitting on  $F^2$  by SHELX-97,<sup>18</sup> and all non-hydrogen atoms were refined with anisotropic thermal parameters. In compound **1**, there are two independent phenylphosphonate groups, which may be conveniently referred to by their constituent phosphorus atoms P1 and P2. The P2 group represents the fully deprotonated form  $\text{C}_6\text{H}_5\text{PO}_3^{2-}$ , in which all oxygen atoms (O6, O7, O8) are coordinated to the silver atoms. The P1 group stands for the hydrogen-bonded  $[\text{C}_6\text{H}_5\text{PO}_3\cdots\text{H}\cdots\text{O}_3\text{PC}_6\text{H}_5]^{3-}$  assembly that lies on a crystallographic 2-axis. The phenyl rings of the two phenylphosphonate groups are each disordered over two orientations such that their carbon atoms (C6–C9, C12–C15, C6'–C9', C12'–C15') are assigned half site-occupancy in least-squares refinement. In addition, the  $\text{CF}_3$  moiety (F1, F2, F3, F4) of  $\text{CF}_3\text{CO}_2^-$  groups is disordered, in which the occupancy ratios of F1, F2, F3, F4 are assigned to 1, 0.6666, 0.6667, 0.6667 in least-squares refinement, respectively (the sum occupancy ratio of F2, F3, and F4 equals 2). In complex **2**, silver atom Ag8 is disordered over two positions of equal site-occupancy, and atom O6 is assigned to a phenylphosphonate hydroxyl group based on the requirement of charge balance. In **3**, atoms O7, O10, O13 belong to phenylphosphonate hydroxyl groups; similarly in **4**, atoms O4 and O8 are assigned to *tert*-butylphosphonate hydroxyl groups. In **6**, silver atoms Ag2 and Ag6 are each disordered over two positions and refined with an assigned site-occupancy ratio of 0.5:0.5. Similarly in **7**, silver atoms Ag8 and Ag9 each exhibit positional disorder and were handled in similar manner, and atom O17 is assigned to a hydroxyl group.

## RESULTS

**Synthesis of Crystalline Complexes.** The first step in the preparative procedure of compounds **1**–**7** follows that reported in our previous work.<sup>17</sup> The crude starting material  $\text{Ag}_2\text{C}_2$  is initially dissolved in a concentrated aqueous solution of  $\text{AgCF}_3\text{CO}_2/\text{AgC}_2\text{F}_5\text{CO}_2$  and  $\text{AgBF}_4$ , the latter being used to provide a sufficiently high concentration of silver(I) ions requisite for dissolving  $\text{Ag}_2\text{C}_2$ . A plausible explanation of the dissolution process is that argentophilicity provides the driving force to transform  $\text{Ag}_2\text{C}_2$  to soluble  $[\text{C}_2@\text{Ag}_n]^{(n-2)+}$  species of indefinite composition. Phenylphosphonic acid or *tert*-butylphosphonic acid is then introduced to the mixed aqueous solution, thereby depositing a pale gray precipitate. Further treatment of the respective solution together with suspended precipitate under hydrothermal condition led to X-ray-quality crystals of **1**–**7**.

**Description of Crystal Structures.**  $\text{Ag}_2\text{C}_2\cdot 2\text{AgCF}_3\text{CO}_2\cdot 2\text{Ag}_2\text{-PhPO}_3\cdot \text{Ag}_3[(\text{PhPO}_3)_2\text{H}]$  (**1**). Compound **1** contains a silver(I) cage  $\text{Ag}_9$  in the shape of a distorted monocapped square antiprism that encapsulates the acetylenediide dianion (Figure 1a). This  $\text{C}_2@\text{Ag}_9$  moiety occupies a crystallographic site of symmetry 2 with atom Ag5 at its apex, and its component atom sets Ag1–Ag2–Ag1a–Ag2a and Ag3–Ag4–Ag3a–Ag4a, which are each coplanar with mean deviation of 0.0006 and 0.0666 Å from the corresponding least-squares plane, respectively, and parallel to each other. The  $\text{C}_2^{2-}$  species

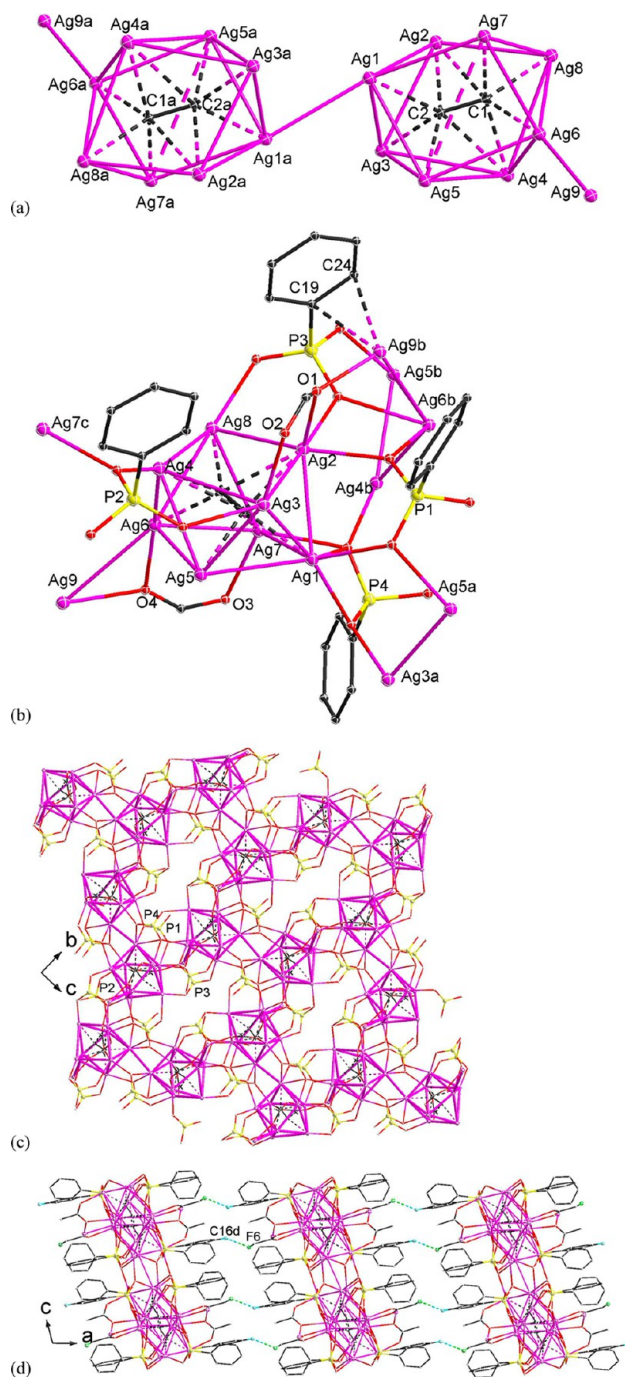


**Figure 3.** (a) Basic building unit in **3** consisting of a  $\text{C}_2@\text{Ag}_8$  cage with an extended arm; two such units are connected by vertex-to-vertex linkage across an inversion center. Ag...Ag distances longer than 3.40 Å are represented by broken lines. Selected bond lengths and distances [Å]:  $\text{C1}\equiv\text{C2}$  1.23(1), Ag...Ag 2.831(1)–3.365(1), Ag9b–C24 2.592(1), Ag9b–C19, 2.754(1). (b) Asymmetric unit in the crystal structure of **3**, showing the single silver cage and the coordination modes of the phosphonate and trifluoroacetate ligands. The H atoms are omitted for clarity. (c) View of the layer structure of **3** parallel to the  $bc$  plane, in which the silver aggregates are linked by phosphonate groups. The phenyl moieties of the phosphonate groups, H, and F atoms are omitted for clarity. (d) Three-dimensional supramolecular framework of **3** generated from the linkage of layers by weak C–H...F hydrogen bonds involving trifluoroacetate and phosphonate groups, which are represented by broken lines. Symmetry codes: (a)  $0.5 - x, 0.5 - y, -z$ ; (b)  $0.5 - x, 0.5 + y, 0.5 - z$ ; (c)  $0.5 - x, -0.5 + y, 0.5 - z$ ; (d)  $-0.5 + x, 0.5 + y, z$ .

enclosed in the silver polyhedron adopts  $\mu_7\text{-}\eta^1, \eta^1, \eta^1, \eta^1, \eta^1, \eta^1, \eta^1$  coordination mode, with silver-ethynide Ag–C mixed ( $\sigma$ ,  $\pi$ ) bonds lying in the range of 2.164(7)–2.462(8) Å, and a  $\pi$ -type<sup>19</sup> Ag2–C1a bond has a length of 2.408(8) Å (Figure 1b).

An edge (Ag2–Ag3) of the Ag<sub>9</sub> square antiprism is bridged by the trifluoroacetate group of type O1–O2. The two independent phosphonate groups (hereafter, the phosphonate groups are conveniently referred to by naming their phosphorus atoms P1 to Pn) adopt different coordination modes to connect with the C<sub>2</sub>@Ag<sub>9</sub> building units: a  $\mu_4\text{-O, O', O'', O''}$  coordination mode for P1 and  $\mu_7\text{-O, O, O', O', O'', O''}$  coordination mode for P2 (Figure 1b). The P1 group is also standing for the hydrogen-bonded [C<sub>6</sub>H<sub>5</sub>PO<sub>3</sub>⋯H⋯O<sub>3</sub>PC<sub>6</sub>H<sub>5</sub>]<sup>3–</sup> assembly that lies on a crystallographic 2-axis (Figure 1c). As shown in Figure 1c, the occupancy ratio of atom H5 and H5a is 0.5, respectively, which can be viewed as one H atom disordered in two positions. The H atom occupies the special positions of site symmetry 2, so that the H atom exhibits orientational disorder.

There are also Ag⋯ $\pi$  interactions<sup>20</sup> between the external silver atom Ag6 and the phenyl rings of the P1 phosphonate groups in  $\eta^2$ -arene coordination mode with Ag–C distances of 2.596(1) (Ag6a–C10) and 2.429(1) Å (Ag6a–C12). The silver cages are connected by the phosphonate groups to form a coordination layer parallel to the *bc* plane (Figure 1d). The bridging trifluoroacetate groups and phenyl moieties of the phosphonate groups protrude from both sides of the coordination layer (Figure 1e).

**4Ag<sub>2</sub>C<sub>2</sub>·4AgCF<sub>3</sub>CO<sub>2</sub>·6Ag<sub>2</sub>PhPO<sub>3</sub>·2AgPhPO<sub>3</sub>H·3H<sub>2</sub>O (2).** Compound **2** is composed of two kinds of silver cages: a pentagonal pyramid (cage A) and a pentagonal bipyramid with a missing vertex (cage B), each enclosing an ethynediide (Figure 2a). The first independent C<sub>2</sub><sup>2–</sup> ligand (C1≡C2) lies close to the base of cage A, being bonded to the vertexes of the pentagonal pyramid through four  $\sigma$ -type and two  $\pi$ -type bonds with Ag–C bond lengths in the range of 2.136(7)–2.375(7) Å. The least-squares deviation of the plane Ag1–Ag2–Ag3–Ag4–Ag5–C1–C2 is 0.081 Å. The second C<sub>2</sub><sup>2–</sup> ligand (C3≡C4) encapsulated by cage B is consolidated by four  $\sigma$ -type and two  $\pi$ -type bonds with Ag–C bond lengths in the range of 2.136(9)–2.368(1) Å. The least-squares deviation of the plane Ag7–Ag9–Ag10–Ag12 is 0.126 Å. These two kinds of silver cages are connected by argentophilic interactions (Ag4⋯Ag12 3.139(1), Ag6⋯Ag7 3.261(1), Ag3⋯Ag10a 3.315(1)) to yield an infinite zigzag chain along the *b* axis, with additional silver atoms of type Ag13 attached to it (Figure 2b). Cross-linkage of such chains through bridging phosphonic groups gives rise to a two-dimensional coordination architecture, with a portion of the Ag⋯Ag bonds further consolidated by trifluoroacetate ligands (Figure 2c).

**Ag<sub>2</sub>C<sub>2</sub>·2AgCF<sub>3</sub>CO<sub>2</sub>·Ag<sub>2</sub>PhPO<sub>3</sub>·3AgPhPO<sub>3</sub>H (3).** The basic building unit in **3** is a Ag<sub>8</sub> distorted square antiprismatic cage that encapsulates a C<sub>2</sub><sup>2–</sup> ligand, with one vertex attached to external atom Ag9 (Figure 3a). Least-squares planes fitted to the tetragonal faces Ag1–Ag5–Ag6–Ag7 and Ag2–Ag3–Ag4–Ag8 show deviations of 0.154 and 0.117 Å, respectively, and they make a dihedral angle of 6.56°. Two such single cages are linked together by the Ag1–Ag1a bond across an inversion center. The encapsulated C1≡C2 moiety is stabilized by six  $\sigma$ - and three  $\pi$ -type interactions with Ag–C bond lengths in the range of 2.195(9)–2.574(8) Å.

The asymmetric unit of compound **3** contains two trifluoroacetate and four phosphonate ligands (Figure 3b). The trifluoroacetate ligands (O1–O2 and O3–O4) each span an Ag⋯Ag edge

(Ag2⋯Ag3 and Ag6⋯Ag7), and both connect with silver atom Ag9 through the  $\mu_3\text{-O, O', O'}$  coordination mode. Ag9 is also involved in  $\eta^2\text{-}\pi$  interaction (Ag9b–C24 and Ag9b–C19) with the phenyl ring of the P3 phosphonate group.

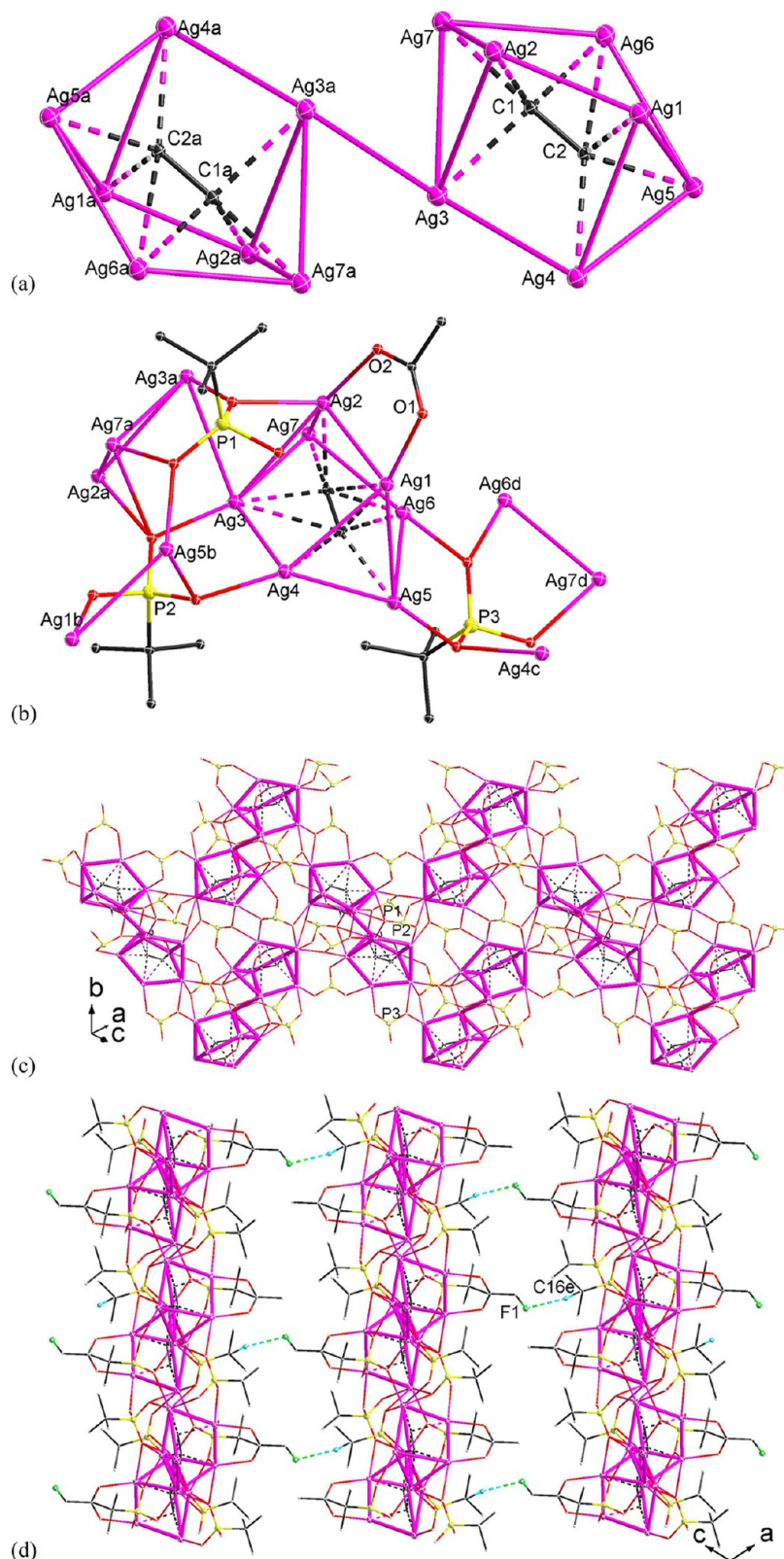
The silver aggregates are connected by the phosphonate groups to form a coordination layer parallel to the *ac* plane (Figure 3c). Weak hydrogen bonds of the type C–H⋯F (C16d⋯F6, 3.401(1) Å) occur between adjacent coordination layers (Figure 3d), thus generating a three-dimensional supra-molecular network.

**Ag<sub>2</sub>C<sub>2</sub>·AgCF<sub>3</sub>CO<sub>2</sub>·Ag<sub>2</sub><sup>t</sup>BuPO<sub>3</sub>·2Ag<sup>t</sup>BuPO<sub>3</sub>H (4).** The asymmetric unit of **4** contains an irregular C<sub>2</sub>@Ag<sub>7</sub> cage, and two inversion-related cages are directly linked by the vertex-to-vertex mode (Figure 4a). The Ag<sub>7</sub> cage can be described as a Ag<sub>5</sub> pentagon capped by two vertexes on the same side; the atom sets Ag3–Ag4–Ag5–Ag6–Ag7 of the pentagonal face are nearly coplanar with a mean deviation of 0.22 Å from the corresponding least-squares plane. The enclosed C<sub>2</sub><sup>2–</sup> species is stabilized by six  $\sigma$ - and one  $\pi$ -type bonding interactions with the Ag vertexes in the range of 2.198(1)–2.431(1) Å. The trifluoroacetate ligand spans the Ag1⋯Ag2 edge in  $\mu_2\text{-O, O'}$  coordination mode, while the three independent phosphonate groups adopt coordination mode  $\mu_4\text{-O, O, O', O'}$  for P1,  $\mu_6\text{-O, O', O', O'', O'', O''}$  for P2, and  $\mu_5\text{-O, O', O', O'', O'', O''}$  for P3, respectively (Figure 4b). The centrosymmetric (C<sub>2</sub>@Ag<sub>7</sub>)<sub>2</sub> aggregates are connected by the phosphonate bridging ligands to form a coordinated layer parallel to the ( $\bar{1}$ , 0, 1) lattice plane (Figure 4c). Such silver layers are further interconnected to yield a 3D supramolecular framework via C–H⋯F hydrogen bonding between the phosphonate ligands and trifluoroacetate groups (Figure 4d).

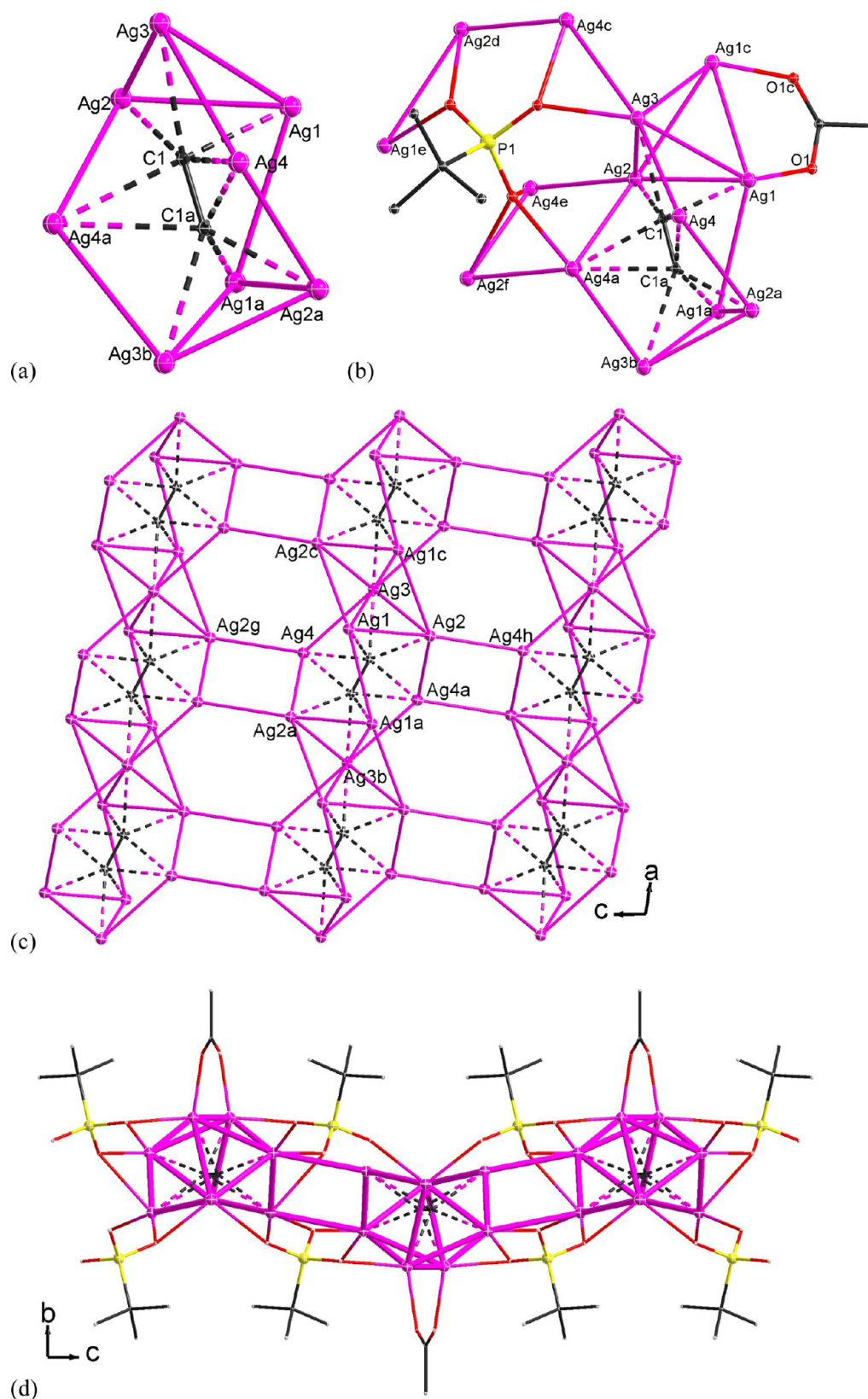
**Ag<sub>2</sub>C<sub>2</sub>·AgCF<sub>3</sub>CO<sub>2</sub>·2Ag<sub>2</sub><sup>t</sup>BuPO<sub>3</sub> (5).** In the crystal structure of **5**, the core is an Ag<sub>8</sub> polyhedron shaped like a screwy jujube pit (Figure 5a). The C1≡C1a moiety enclosed in the polyhedron is stabilized by six  $\sigma$ - and two  $\pi$ -type Ag–C bonds with its bond length in the range of 2.246(2)–2.535(2) Å. In the asymmetric unit of **5**, there is one independent phosphonate group and a half trifluoroacetate ligand (Figure 5b). The trifluoroacetate ligand spans the Ag1⋯Ag1c edge through the  $\mu_2\text{-O, O'}$  mode, whereas the phosphonate ligand connects to the silver skeleton via  $\mu_7\text{-O, O, O', O', O'', O'', O''}$  coordination mode. The screwy jujube pit-like silver polyhedra share vertexes of the type Ag3, together with further connection of Ag1⋯Ag2c and Ag1c⋯Ag2, to form a helical column along the *a* direction (Figure 5c). A parallel arrangement of such silver columns is linked by Ag⋯Ag interactions (Ag2⋯Ag4h) to form an argentophilic layer, which is further consolidated by the trifluoroacetate ligands and phosphonate ligands (Figure 5d).

**2Ag<sub>2</sub>C<sub>2</sub>·2AgC<sub>2</sub>F<sub>5</sub>CO<sub>2</sub>·4Ag<sub>2</sub>PhPO<sub>3</sub>·H<sub>2</sub>O (6).** In the crystal structure of **6**, there exist four kinds of C<sub>2</sub>@Ag<sub>6</sub> irregular polyhedra (Figure 6a). The moieties C1≡C2, C3≡C4, C7≡C8 are each coordinated to its polyhedral vertexes via the  $\mu_6\text{-}\eta^1, \eta^1, \eta^1, \eta^2, \eta^2, \eta^2$  mode; meanwhile, the moiety C5≡C6 adopts the  $\mu_6\text{-}\eta^1, \eta^1, \eta^1, \eta^1, \eta^1, \eta^2$  coordination mode. The Ag–C bonds length are in the range of 2.132(1)–2.688(1) Å. The polyhedra labeled A and B share vertexes of type Ag9 and Ag14 with additional Ag12⋯Ag17d and Ag13⋯Ag16 contacts to generate an infinite silver column ABAB⋯ running along the *b* direction (Figure 6b). Similarly, polyhedra C and D sharing silver atoms Ag20 and Ag24 have additional Ag22⋯Ag25 and Ag27⋯Ag19a contacts, yielding an infinite silver column CDCD⋯ alongside ABAB⋯. These two types of parallel columns are cross-linked by argentophilic interactions (Ag12⋯Ag22 3.167(1) Å,





**Figure 4.** (a) Centrosymmetric aggregate  $(C_2@Ag_7)_2$  in **4** composed of two single silver cages, each taking the shape of a pentagon with two caps on the same side. Selected bond lengths and distances [Å]:  $C1\equiv C2$  1.24(2),  $Ag\cdots Ag$  2.789(2)–3.351(2). (b) Asymmetric unit in the crystal structure of **4**, showing the single silver cage, and the coordination modes of the phosphonate groups and trifluoroacetate groups. The H atoms are omitted for clarity. (c) Perspective view of the 2D coordination network of **4** parallel to the  $(1, 0, 1)$  lattice plane constructed from the silver aggregate  $(C_2@Ag_7)_2$  connected by phosphonate bridges. The H and F atoms and the  $C(CH_3)_3$  moieties of the phosphonate groups are omitted for clarity. (d) View of 3D supramolecular framework of **4**, showing the linkage of silver chains by  $C-H\cdots F$  hydrogen bonds involving phosphonate ligands and trifluoroacetate groups. (The  $C-H\cdots F$  interactions are represented by broken yellow lines;  $F1\cdots C16e = 3.573(1)$  Å). Symmetry codes: (a)  $-x, 2-y, -z$ ; (b)  $0.5-x, 0.5+y, 0.5-z$ ; (c)  $0.5-x, -0.5+y, 0.5-z$ ; (d)  $-x, 1-y, -z$ ; (e)  $0.5+x, 1.5-y, -0.5+z$ .





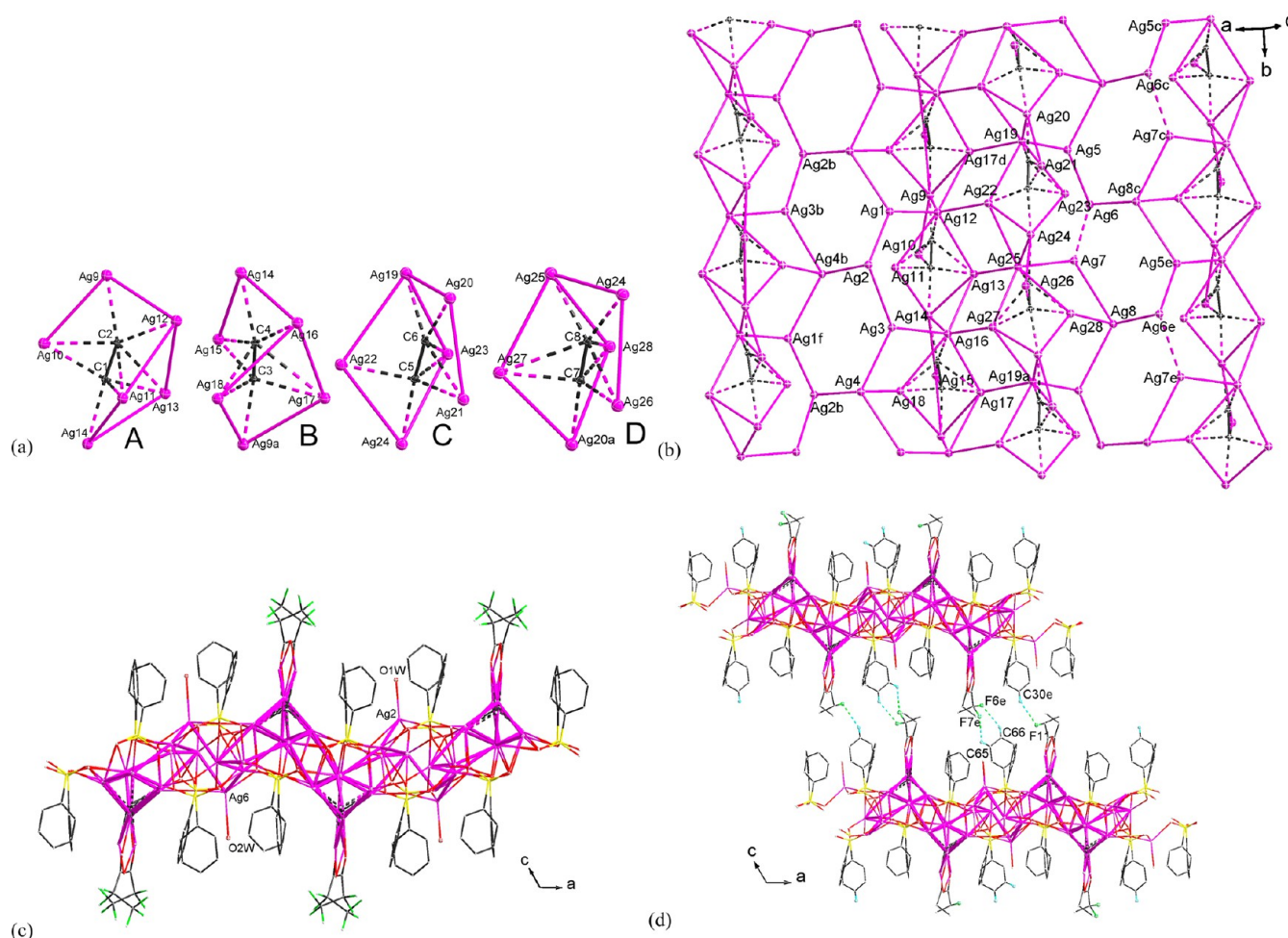


**Figure 6.** (a) Four types of irregular polyhedra existing in the compound **6**. Selected bond lengths and distances [Å]: C1≡C2 1.24(2), C3≡C4 1.24(2), C5≡C6 1.23(2), C7≡C8 1.22(2), Ag⋯Ag 2.769(1)–3.334(1). (b) Perspective view of argentophilic layer parallel to the *ab* plane, showing two sets of silver columns ABAB⋯ and CDCD⋯. The Ag6⋯Ag7 distance represented by a broken line is 3.42, which is longer than 3.4 Å (twice the van der Waals radius of silver). (c) View of the coordinated argentophilic layer along the *b* direction. The H atoms are omitted for clarity. (d) Linkage of silver layers by hydrogen bonds to give a three-dimensional supramolecular framework in **6** (the C–H⋯F interactions are presented by broken yellow lines: C30e⋯F11 = 3.494 Å; C65⋯F7e = 3.285 Å; C66⋯F6e = 3.438 Å). All irrespective H atoms, F atoms are omitted for clarity. Symmetry codes: (a) *x*, 1 + *y*, *z*; (b) 1 − *x*, −0.5 + *y*, 1.5 − *z*; (c) −*x*, −0.5 + *y*, 1.5 − *z*; (d) *x*, −1 + *y*, *z*; (e) −*x*, −0.5 + *y*, 1.5 − *z*; (f) 1 − *x*, 0.5 + *y*, 1.5 − *z*.

Ag13⋯Ag26 3.153(1) Å, Ag16⋯Ag27 3.156(1) Å, Ag17d⋯Ag19 3.244(1) Å) to generate a thick column (Figure 6b). On opposite sides of each thick silver column, there are two sets of silver chains Ag1–Ag2–Ag3–Ag4 and Ag5–Ag6–Ag7–Ag8 connected to the silver aggregates via argentophilic interactions. The external silver atoms Ag1–Ag8 are acting like bridges to link up other sets of silver columns via bond type Ag2⋯Ag4b (2.797(1) Å) and Ag6⋯Ag8c (2.954(1) Å); thus an argentophilic layer parallel to the *ab* plane is formed (Figure 6b). The argentophilic layer is further consolidated by the pentafluoropropionate ligands and phosphonate ligands (Figure 6c). The aqua ligands O1W and O2W are attached to the silver skeleton by silver atoms Ag2 and Ag6 respectively. Between the adjacent argentophilic layers, there is existing C–H⋯F hydrogen bonding involving pentafluoropropionate ligands and phosphonate ligands; thus a three-dimensional supramolecular architecture is formed (Figure 6d).

**1.5Ag<sub>2</sub>C<sub>2</sub>·6AgC<sub>2</sub>F<sub>5</sub>CO<sub>2</sub>·Ag<sub>2</sub>PhCH<sub>2</sub>PO<sub>3</sub>·AgPhCH<sub>2</sub>PO<sub>3</sub>H·6H<sub>2</sub>O (7).** There exist two kinds of C<sub>2</sub>@Ag<sub>8</sub> irregular polyhedra in compound **7** (Figure 7a). Silver cage A is composed of a triangular face (Ag4–Ag5–Ag6) and a pentagonal face (Ag1–Ag2–Ag3–Ag7–Ag8), which is coplanar with a mean deviation

of 0.1947 Å from the corresponding least-squares plane, and they make a dihedral angle of 3.65°. The ethynide species C1≡C2 located in cage A is stabilized by six σ- and two π-type bonding interactions with Ag–C bond lengths in the range of 2.136(7)–2.375(7) Å. Centrosymmetric silver cage B is in the shape of a distorted square antiprism, with an encapsulated ethynide species C3≡C3a stabilized by six σ- and two π-type bonding interactions (Ag–C 2.147(9)–2.471(1) Å). The tetragonal faces Ag9–Ag10–Ag9a–Ag10a and Ag11–Ag12–Ag11a–Ag12a of cage B are parallel to each other, with mean deviations of 0.239 and 0.203 Å from the corresponding least-squares plane, respectively. The polyhedra A and B are connected by the trifluoroacetate ligands and phosphonate ligands to generate an infinite composite silver chain A<sub>2</sub>BA<sub>2</sub>B⋯ running along the *c* direction (Figure 7b). The silver chain is also consolidated by Ag⋯π interactions, including η<sup>2</sup>-π type (Ag9–C7 = 2.636(1) Å and Ag9–C8 = 2.400(1) Å) and η<sup>3</sup>-π type (Ag1b–C14 = 2.647(1) Å, Ag1b–C15 = 2.386(1) Å, and Ag1b–C16 = 2.779(1) Å). Aqua ligand O2W serves as a bridge between the silver chains, thus forming a three-dimensional coordination architecture (Ag8–O2W = 2.359(8) Å, O2W–Ag7c



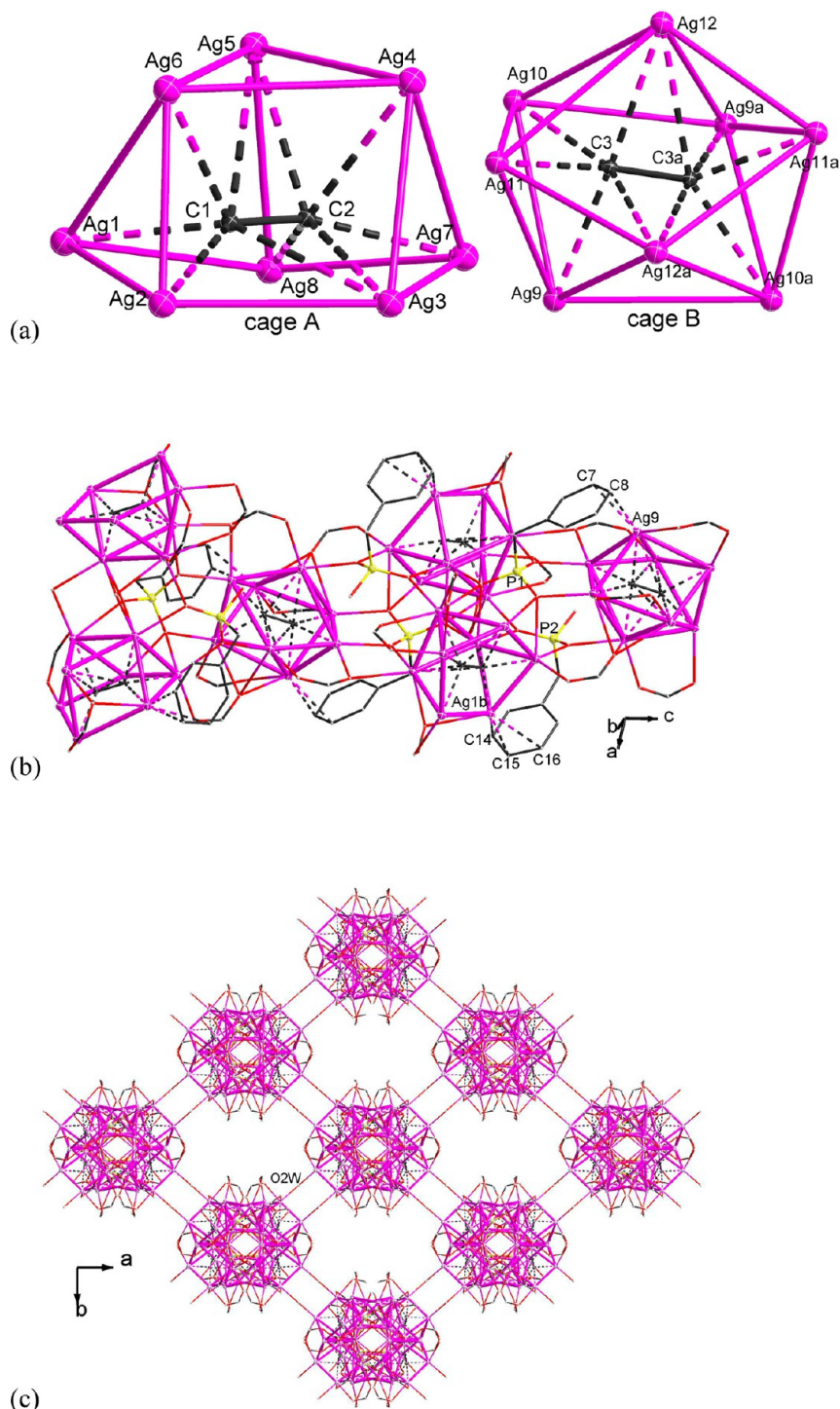


**Figure 7.** (a) Two types of irregular polyhedra existing in the compound 7. Selected bond lengths and distances [ $\text{\AA}$ ]:  $C1\equiv C2$  1.24(1),  $C3\equiv C3a$  1.24(2),  $Ag\cdots Ag$  2.794(1)–3.354(1). (b) Perspective view of coordination silver chain constructed of silver cages in the form of  $A_2BA_2B\cdots$ . The unimportant atoms are omitted for clarity. (c) Three-dimensional coordination architecture of 7 generated from the cross-linkage of silver chains by coordination with aqua ligands O2W. The unimportant atoms are omitted for clarity. Symmetry codes: (a)  $1-x, y, 0.5-z$ ; (b)  $1-x, 1-y, -z$ ; (c)  $0.5-x, 1.5-y, -z$ .

$= 2.555(7)$   $\text{\AA}$ ) (Figure 7c). Of the remaining five independent water molecules, O1W and O3W function as aqua ligands, and the rest (O4W, O5W, and O6W) occupy sites in the crystal lattice.

## DISCUSSION

**The Role and Coordination Modes of Phosphonate Ligands.** As mentioned before,  $C_2@Ag_n$  ( $n = 6-9$ ) species

formed from the dissolution of  $Ag_2C_2$  in a concentrated aqueous solution of silver salts are quite labile. In the present study, such cage species are consolidated by the phosphonate groups and perfluorocarboxylate ligands to give a variety of crystalline silver(I) complexes. Compounds 1–6 are found to exhibit coordination layer structures, while compound 7 features a three-dimensional coordination network. The structure of compound 2 exhibits an

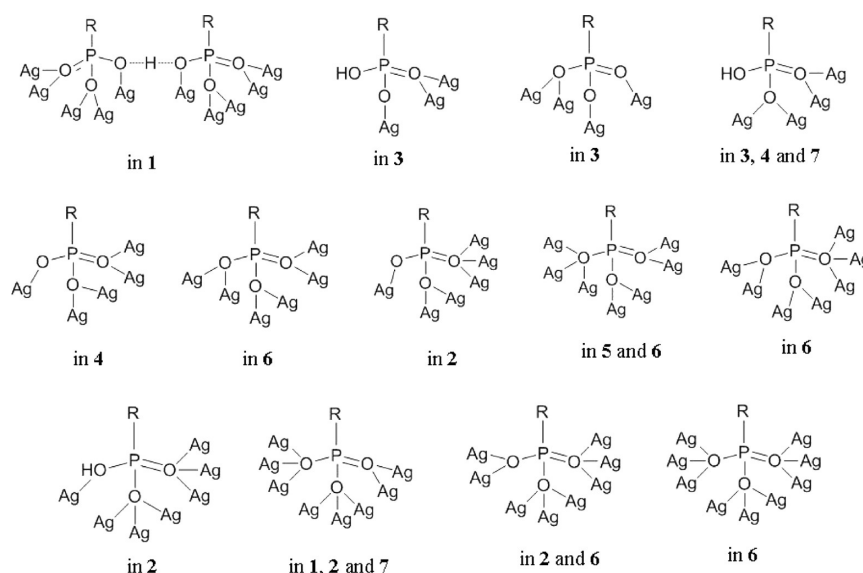


Figure 8. Coordination modes of phosphonate ligands in 1–7.

argentophilic chain, and compounds 5 and 6 are each composed of argentophilic layers. Under hydrothermal conditions, phosphonic acid as a reactant underwent different degrees of deprotonation, yielding distinguishable phosphonate ligands of the types  $\text{RPO}_3\text{H}^-$ ,  $\text{RPO}_3^{2-}$ , and  $[\text{RPO}_3\cdots\text{H}\cdots\text{O}_3\text{PR}]^{3-}$  that adopt a rich variety of coordination modes to bind multiple silver(I) centers (Figure 8). Notably, the hydroxyl group in the  $\text{RPO}_3\text{H}^-$  ligand was found to coordinate to only one silver atom.

Notably, if different species generated from the same phosphonic acid precursor are considered as distinguishable anions, compounds 1–4 and 7 can be considered as silver(I) quadruple salts, whereas 5 and 6 are triple salts.

**Synthesis Controlled by Variation of Mole Ratios of Reactants.** It should be noted that compounds 1–3 were synthesized under the same reaction condition with different mole ratios of reactants. Likewise, for compounds 4, 5, variation in the mole ratios of reactants gave rise to different products. In the  $\text{Ag}_2\text{C}_2$ -containing reaction system, the concentration of silver(I) ions was kept very high to achieve the requisite for dissolving  $\text{Ag}_2\text{C}_2$ , which was handled in the wet form to avoid explosion. After establishment of the structural formula of  $\text{Ag}_2\text{C}_2\cdot 2\text{AgCF}_3\text{CO}_2\cdot 2\text{Ag}_2\text{PhPO}_3\cdot \text{Ag}_3[(\text{PhPO}_3)_2\text{H}]$  (1) and  $4\text{Ag}_2\text{C}_2\cdot 4\text{AgCF}_3\text{CO}_2\cdot 6\text{Ag}_2\text{PhPO}_3\cdot 2\text{AgPhPO}_3\cdot 3\text{H}_2\text{O}$  (2), we realized that the  $\text{Ag}_2\text{C}_2\cdot \text{AgCF}_3\text{CO}_2\cdot \text{PhPO}_3^{2-}$  component ratios are 1:2:4 and 1:1:2, respectively, which agree well with the mole ratios of the reactants employed in the syntheses. The mole ratios of  $\text{Ag}_2\text{C}_2\cdot \text{AgCF}_3\text{CO}_2\cdot \text{PhPO}_3^{2-}$  in both  $\text{Ag}_2\text{C}_2\cdot 2\text{AgCF}_3\text{CO}_2\cdot 2\text{Ag}_2\text{PhPO}_3\cdot \text{Ag}_3[(\text{PhPO}_3)_2\text{H}]$  (1) and  $\text{Ag}_2\text{C}_2\cdot 2\text{AgCF}_3\text{CO}_2\cdot \text{Ag}_2\text{PhPO}_3\cdot 3\text{AgPhPO}_3\cdot \text{H}$  (3) are 1:2:4, but the phosphonate groups in these two compounds take the forms  $2\text{Ag}_2\text{PhPO}_3\cdot \text{Ag}_3[(\text{PhPO}_3)_2\text{H}]$  and  $\text{Ag}_2\text{PhPO}_3\cdot 3\text{AgPhPO}_3\cdot \text{H}$ , respectively. Associated with their synthetic procedures (compound 3 was synthesized in a manner similar to that of compound 1 using 80 mg of phenylphosphonic acid instead of 60 mg), we can deduce a plausible explanation that deprotonation of phenylphosphonic acid is hindered by a higher concentration of it in the reactant solution. This rationale can also account for the formation of compounds  $\text{Ag}_2\text{C}_2\cdot \text{AgCF}_3\text{CO}_2\cdot \text{Ag}_2^t\text{BuPO}_3\cdot 2\text{Ag}^t\text{BuPO}_3\cdot \text{H}$  (4) and  $\text{Ag}_2\text{C}_2\cdot \text{AgCF}_3\text{CO}_2\cdot 2\text{Ag}_2^t\text{BuPO}_3$  (5). Compound 5 was synthesized in manner similar to that of compound 4 by slightly reducing the amount of *tert*-butylphosphonic acid employed from 60 to 40 mg.

## CONCLUSION

In summary, we have successfully incorporated phosphonate ligands into the silver-ethynediide system via hydrothermal synthesis to obtain a series of seven new silver(I) multiple salts of  $\text{Ag}_2\text{C}_2$ . Compounds 1–3 were synthesized at the same reaction temperature with the same reactants by slightly changing their mole ratios. The same procedure was used likewise to obtain compounds 4, 5. Complexes 1–6 exhibit coordination layer structures, in which the  $\text{C}_2@ \text{Ag}_9$  cages (found in 1), argentophilic chains (2),  $(\text{C}_2)_2@ \text{Ag}_{18}$  aggregates (in 3),  $(\text{C}_2)_2@ \text{Ag}_{14}$  aggregates (in 4), and argentophilic layers (in 5 and 6) are linked or consolidated by the phosphonate ligands, while compound 7 has a three-dimensional coordination network. As demonstrated in this study, the incorporation of phosphonate ligands into the silver-ethynediide system significantly enriches its structural chemistry, and hydrothermal synthetic methods show good promise in the generation of new types of silver phosphonates.

## ASSOCIATED CONTENT

### Supporting Information

X-ray crystallographic files (CIF) of complexes 1–7 and selected bond lengths (Å). This material is available free of charge via the Internet at <http://pubs.acs.org>.

## AUTHOR INFORMATION

### Corresponding Author

\*E-mail: [tcwmak@cuhk.edu.hk](mailto:tcwmak@cuhk.edu.hk)

### Notes

The authors declare no competing financial interest.

## ACKNOWLEDGMENTS

We gratefully acknowledge financial support by the Hong Kong Research Grants Council (GRF CUHK 402710) and the Wei Lun Foundation, as well as the award of a Studentship to T.H. by The Chinese University of Hong Kong.

## REFERENCES

- (1) Mak, T. C. W.; Zhao, X.-L.; Wang, Q.-M.; Guo, G.-C. *Coord. Chem. Rev.* **2007**, *251*, 2311–2333.



- (2) (a) Zhao, L.; Mak, T. C. W. *J. Am. Chem. Soc.* **2004**, *126*, 6852–6853. (b) Zhao, L.; Du, M.; Mak, T. C. W. *Asian J. Chem.* **2007**, *2*, 1240–1257. (c) Gao, C.-Y.; Zhao, L.; Wang, M.-X. *J. Am. Chem. Soc.* **2012**, *134*, 824–827. (d) Hu, T.; Zhao, L.; Mak, T. C. W. *Organometallics* **2012**, *31*, 7539–7547.
- (3) (a) Mak, T. C.; Zhao, L.; Zhao, X. L. Supramolecular Assembly of Silver(I) Complexes with Argentophilic and Silver...Carbon Interactions. In *The Importance of Pi-Interactions in Crystal Engineering—Frontiers in Crystal Engineering III*; Tiekink, E. R. T., Zukerman-Schpector, J., Eds.; Wiley: Chichester, 2012; Chapter 13, pp 323–366. (b) Xie, Y.-P.; Al-Thabaiti, S. A.; Mokhtar, M.; Mak, T. C. W. *Inorg. Chem. Commun.* **2013**, *31*, 54–57. (c) Hau, S. C. K.; Cheng, P.-S.; Mak, T. C. W. *Polyhedron* **2013**, *52*, 992–1008. (d) Cheng, P.-S.; Marivel, S.; Zang, S.-Q.; Gao, G.-G.; Mak, T. C. W. *Cryst. Growth Des.* **2012**, *12*, 4519–4529. (e) Hu, T.; Mak, T. C. W. *Organometallics* **2012**, *32*, 202–208. (f) Xie, Y.-P.; Mak, T. C. W. *Chem. Commun.* **2012**, *48*, 1123–1125. (g) Xie, Y.-P.; Wang, H.; Mak, T. W. *J. Cluster Sci.* **2012**, *23*, 727–736.
- (4) (a) Hau, S. C. K.; Cheng, P.-S.; Mak, T. C. W. *J. Am. Chem. Soc.* **2012**, *134*, 2922–2925. (b) Zhang, T.; Song, H.; Dai, X.; Meng, X. *Dalton Trans.* **2009**, 7688–7694.
- (5) (a) Rais, D.; Yau, J.; Mingos, D. M. P.; Vilar, R.; White, A. J. P.; Williams, D. J. *Angew. Chem., Int. Ed.* **2001**, *40*, 3464–3467. (b) Gruber, F.; Jansen, M. *Angew. Chem., Int. Ed.* **2010**, *122*, 5044–5046.
- (6) (a) Mak, T. C. W.; Zhao, L. *Asian J. Chem.* **2007**, *2*, 456–467. (b) Zhao, L.; Wan, C.-Q.; Han, J.; Chen, X.-D.; Mak, T. C. W. *Chem.-Eur. J.* **2008**, *14*, 10437–10444.
- (7) (a) Zhang, Z.; Li, B.; Meng, X.; Yin, X.; Zhang, T. *Dalton Trans.* **2013**. (b) Bian, S. D.; Wang, Q. M. *Chem. Commun.* **2008**, 5586–5588. (c) Rais, D.; Mingos, D. M. P.; Vilar, R.; White, A. J. P.; Williams, D. J. *J. Organomet. Chem.* **2002**, *652*, 87–93.
- (8) (a) Plabst, M.; McCusker, L. B.; Bein, T. *J. Am. Chem. Soc.* **2009**, *131*, 18112–18118. (b) Wu, J.; Hou, H.; Han, H.; Fan, Y. *Inorg. Chem.* **2007**, *46*, 7960–7970. (c) Ma, T.-Y.; Yuan, Z.-Y. *Chem. Commun.* **2010**, *46*, 2325–2327.
- (9) (a) Zheng, Y.-Z.; Evangelisti, M.; Tuna, F.; Winpenny, R. E. P. *J. Am. Chem. Soc.* **2011**, *134*, 1057–1065. (b) Cremades, E.; Gómez-Coca, S.; Aravena, D.; Alvarez, S.; Ruiz, E. J. *J. Am. Chem. Soc.* **2012**, *134*, 10532–10542. (c) Yang, B.-P.; Prosvirin, A. V.; Guo, Y.-Q.; Mao, J.-G. *Inorg. Chem.* **2008**, *47*, 1453–1459. (d) Wang, P.-F.; Bao, S.-S.; Zhang, S.-M.; Cao, D.-K.; Liu, X.-G.; Zheng, L.-M. *Eur. J. Inorg. Chem.* **2010**, *2010*, 895–901.
- (10) (a) Maillat, C.; Janvier, P.; Pipelier, M.; Praveen, T.; Andres, Y.; Bujoli, B. *Chem. Mater.* **2001**, *13*, 2879–2884. (b) Clearfield, A.; Sharma, C. V. K.; Zhang, B. *Chem. Mater.* **2001**, *13*, 3099–3112. (c) Shi, X.; Zhu, G.; Qiu, S.; Huang, K.; Yu, J.; Xu, R. *Angew. Chem., Int. Ed.* **2004**, *116*, 6644–6647.
- (11) Carraro, M.; Sartorel, A.; Scorrano, G.; Maccato, C.; Dickman, M. H.; Kortz, U.; Bonchio, M. *Angew. Chem., Int. Ed.* **2008**, *47*, 7275–7279.
- (12) (a) Kim, S.; Dawson, K. W.; Gelfand, B. S.; Taylor, J. M.; Shimizu, G. K. H. *J. Am. Chem. Soc.* **2013**, *135*, 963–966. (b) Colodrero, R. M. P.; Olivera-Pastor, P.; Losilla, E. R.; Hernández-Alonso, D.; Aranda, M. A. G.; León-Reina, L.; Rius, J.; Demadis, K. D.; Moreau, B.; Villemin, D.; Palomino, M.; Rey, F.; Cabeza, A. *Inorg. Chem.* **2012**, *51*, 7689–7698. (c) Colodrero, R. M. P.; Papathanasiou, K. E.; Stavgianoudaki, N.; Olivera-Pastor, P.; Losilla, E. R.; Aranda, M. A. G.; León-Reina, L.; Sanz, J.; Sobrados, I.; Choquesillo-Lazarte, D.; García-Ruiz, J. M.; Atienzar, P.; Rey, F.; Demadis, K. D.; Cabeza, A. *Chem. Mater.* **2012**, *24*, 3780–3792.
- (13) (a) Zhou, T.-H.; Yi, F.-Y.; Li, P.-X.; Mao, J.-G. *Inorg. Chem.* **2009**, *49*, 905–915. (b) Tang, S.-F.; Song, J.-L.; Li, X.-L.; Mao, J.-G. *Cryst. Growth Des.* **2006**, *6*, 2322–2326. (c) Mao, J.-G. *Coord. Chem. Rev.* **2007**, *251*, 1493–1520. (d) Wang, C.-M.; Wu, Y.-Y.; Chang, Y.-W.; Lii, K.-H. *Chem. Mater.* **2008**, *20*, 2857–2859. (e) Song, J.-L.; Mao, J.-G. *Chem.-Eur. J.* **2005**, *11*, 1417–1424.
- (14) (a) Xie, Y.-P.; Mak, T. C. W. *J. Am. Chem. Soc.* **2011**, *133*, 3760–3763. (b) Xie, Y.-P.; Mak, T. C. W. *Angew. Chem., Int. Ed.* **2012**, *51*, 8783–8786. (c) Xie, Y.-P.; Mak, T. C. W. *Inorg. Chem.* **2012**, *51*, 8640–8642.
- (15) Zhao, X.-L.; Mak, T. C. W. *Inorg. Chem.* **2010**, *49*, 3676–3678.
- (16) (a) Guo, G.-C.; Zhou, G.-D.; Wang, Q.-G.; Mak, T. C. W. *Angew. Chem., Int. Ed.* **1998**, *37*, 630–632. (b) Wang, Q.-M.; Mak, T. C. W. *J. Am. Chem. Soc.* **2001**, *123*, 1501–1502.
- (17) *CrystalClear, Version 1.3.5*; Rigaku Corp.: Woodlands, TX, 1999.
- (18) Sheldrick, G. M. *SHELXTL, Crystallographic Software Package, Version 5.1*; Bruker-AXS: Madison, WI, 1998.
- (19) In our working model, the terminal carbon atom bearing the negative charge draws neighboring Ag(I) atoms together to facilitate the onset of argentophilic interactions, such that the multinuclear silver-ethynide binding interaction is considered to be mainly ionic with minor covalent  $\sigma$ - and  $\pi$ -type components. Therefore, the designation of “silver-ethynide bonds” of  $\sigma$ - or mixed ( $\sigma$ ,  $\pi$ )-type should not be taken as normal covalent or coordination bonds.
- (20) (a) Amma, E. L.; Griffith, E. A. H. *J. Am. Chem. Soc.* **1971**, *93*, 3167–3172. (b) Wang, Q.-M.; Mak, T. C. W. *J. Am. Chem. Soc.* **2001**, *123*, 7594–7600. (c) Zhao, L.; Mak, T. C. W. *Organometallics* **2007**, *26*, 4439–4448. (d) Zheng, X.-F.; Zhu, L.-G. *Cryst. Growth Des.* **2009**, *9*, 4407–4414.